Is the Aromatic Fragment of Piano-Stool Ruthenium Compounds an Essential Feature for Anticancer Activity? The Development of New Ru^{II}-[9]aneS_3 Analogues

Barbara Serli,[a] Ennio Zangrando,[a] Teresa Gianferrara,[b] Claudine Scolaro,[c] Paul J. Dyson,[c] Alberta Bergamo,[d] and Enzo Alessio*[a]

Keywords: Antitumor agents / Facial coordination / Half-sandwich complexes / Ruthenium / S ligands

New half-sandwich Ru^{II}-[9]aneS_3 complexes ([9]aneS_3 = 1,4,7-trithiacyclononane), namely [$RuCl_2$(PTA)([9]aneS_3)] (**4**), [RuCl(PTA)$_2$([9]aneS_3)][OTf] (**5**), [RuCl(en)([9]aneS_3)][OTf] (**6**), [RuCl(enac)([9]aneS_3)][OTf] (**7**), [RuCl(bipy)([9]aneS_3)][OTf] (**8**), and [Ru(dmso-S)(bipy)([9]aneS_3)][OTf]$_2$ (**9**) [PTA = 1,3,5-triaza-7-phosphaadamantane; enac = 1,2-bis-(isopropyleneimino)ethane; OTf = $CF_3SO_3^-$] were prepared from Ru-[9]aneS_3–dmso precursors and structurally characterized, both in solution and in the solid state by X-ray crystallography. Some of them are analogs of known cytotoxic organometallic Ru^{II}-(η^6-arene) and Ru^{II}-(η^5-cyclopentadienyl) compounds, in which the aromatic fragment is replaced by the sulfur macrocycle 1,4,7-trithiacyclononane, while the rest of the coordination sphere is left unchanged. Similarly to the aromatic analogs for which data are available, in aqueous solution the Ru-[9]aneS_3 complexes (with the exception of **5**) hydrolyze a chloride (or a dmso in the case of **9**) to give the corresponding aquo species. This process is rapidly reversed in the presence of free chloride, and coordination of phosphate is likely to occur to the aquo species in phosphate buffered solutions at physiological pH. Preliminary in vitro tests performed on complexes **4**–**6** against the mouse adenocarcinoma cancer cell line (TS/A) and the human mammary normal cell line (HBL-100) showed that, in general, the Ru-[9]aneS_3 compounds have a cytotoxicity comparable to that of the corresponding organometallic analogs. These results suggest that the aromatic fragment of the piano-stool Ru^{II} compounds is not an essential feature for the in vitro anticancer activity, and it might be effectively replaced by another face-capping ligand with a low steric demand, such as [9]aneS_3.

Introduction

The field of anticancer ruthenium drugs is attracting growing interest because some compounds have proved to have very encouraging pharmacological profiles;[1] in particular, they show in vivo activity against tumors that are resistant to cisplatin and carboplatin and a generally lower toxicity (and hence side-effects) than platinum drugs. The most advanced representatives of this new class of anticancer agents are the two Ru^{III} coordination compounds KP1019 {[indH][*trans*-$RuCl_4$(ind)$_2$]; ind = indazole}, developed in the Eighties by Keppler and co-workers,[2] and NAMI-A {[imH][*trans*-$RuCl_4$(dmso-S)(im)]; im = imidazole}, developed in the Nineties by some of us.[3] NAMI-A is selectively active against metastases of solid tumors,[4] while KP1019 is active against colorectal tumors.[5] Both compounds were recently tested on humans because of their promising activities against platinum-resistant malignancies; NAMI-A has completed a phase-I trial and is scheduled to begin phase-II trials soon,[6] while KP1019 is currently in phase-I trials.[7] Contrary to platinum anticancer compounds, the activity of NAMI-A seems to be unrelated to direct cytotoxicity.

More recently, an entirely different class of Ru^{II} compounds developed by Sadler and co-workers has shown very promising anticancer activity both in vitro and in vivo.[8] This class comprises organometallic half-sandwich Ru^{II}–arene complexes of the type [RuCl(en)(η^6-arene)][PF_6] (arene = benzene, *p*-cymene, tetrahydroanthracene, dihydroanthracene, biphenyl), also called "piano-stool" complexes because of their geometry (Figure 1). Such complexes exhibit IC_{50} values (IC_{50} = concentration of compound that kills 50% of cell population) in vitro in the range 6–200 μM against a human ovarian cancer cell line, compared with values of 0.5 μM for cisplatin and 6 μM for carboplatin.[8] The initial in vitro and in vivo studies sug-

[a] Dipartimento di Scienze Chimiche, University of Trieste, Via L. Giorgieri 1, 34127 Trieste, Italy
E-mail: alessi@univ.trieste.it
[b] Dipartimento di Scienze Farmaceutiche, University of Trieste, Piazzale Europa 1, 34127 Trieste, Italy
[c] Institut des Sciences et Ingénierie Chimiques, Ecole Polytechnique Fédérale de Lausanne (EPFL), 1015 Lausanne, Switzerland
[d] Callerio Foundation Onlus, Via A. Fleming 22–31, 34127 Trieste, Italy
Supporting information for this article is available on the WWW under http://www.eurjic.org or from the author.

gested that the most active complexes contain the most hydrophobic η^6-arene ligands. For example, [RuCl(en)(η^6-biphenyl)][PF_6] is active in the A2780 human ovarian cancer xenograft and is not cross-resistant in the A2780cis xenograft.[9] The target for these Ru^{II}–arene complexes might be DNA.[10] Investigations with natural DNA in a cell-free medium indicated that they bind preferentially to guanine residues; binding involves mono-functional coordination to G N7 (after chloride release) and noncovalent, hydrophobic interactions between the arene ligand and DNA, which may include arene intercalation and minor groove binding.[11]

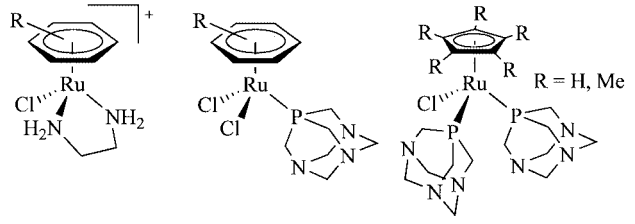

Figure 1. Schematic drawings of the cytotoxic organometallic piano-stool compounds. [RuCl(en)(η^6-arene)]$^+$, [$RuCl_2$(PTA)(η^6-arene)], and [RuCl(PTA)$_2$(η^5-C_5R_5)].

The biological activities of other piano-stool organometallic Ru^{II} complexes have been investigated at different levels. The 1,3,5-triaza-7-phosphaadamantane (PTA) complex [$RuCl_2$(PTA)(η^6-*p*-cymene)] (Figure 1) has proved to have in vitro pH-dependent DNA binding properties and to induce apoptosis in neuroblastoma cells at nanomolar concentrations.[12] It was observed that for the Ru^{II}–arene PTA complexes loss of the arene can occur on binding to an oligonucleotide.[13] In vivo, [$RuCl_2$(PTA)(η^6-*p*-cymene)] has been found to be capable of inhibiting lung metastases in CBA mice bearing the MCa mammary carcinoma, reducing both their number and weight.[14] Related compounds have also been shown to exhibit antimicrobial properties.[15] In vitro anticancer properties have been demonstrated for the compounds [RuCl(BESE)(η^6-*p*-cymene)]$^+$ [BESE = $EtS(O)(CH_2)_2S(O)Et$][16] and [RuCl(PTA)$_2$(η^5-C_5Me_5)] (interestingly, the corresponding η^5-C_5H_5 complex is not cytotoxic, perhaps due to its lower lipophilicity).[17] In addition, [$RuCl_2$(Y)(η^6-C_6H_6)] compounds (Y = dmso, 3-aminopyridine, aminoguanidine, *p*-aminobenzoic acid) have been shown to have topoisomerase II poisoning and in vitro anticancer activity (at 100–300 μM concentrations); interaction of these compounds with DNA in vitro and formation of ternary cleavage complexes of topo II-drug-DNA has been demonstrated.[18] Coordination of the known anticancer agent 1-β-hydroxyethyl-2-methyl-5-nitroimidazole (metronidazole) to the Ru^{II}–benzene fragment affords [$RuCl_2$(metronidazole)(η^6-C_6H_6)], which has superior selective cytotoxicity to metronidazole itself and topoisomerase II activity.[19] Sheldrick and co-workers have published some ruthenium(II)–arene compounds with alanine- and guanine-derived co-ligands,[20] and while their anticancer activity was not included in the report, they were found to be cytotoxic towards P388 leukaemia cells.[21]

All these organometallic compounds are characterized by the presence of a face-capping aromatic ligand, either neutral (η^6-arene) or negatively charged (η^5-cyclopentadienyl), firmly bound to ruthenium. We were interested to establish whether the aromatic fragment is an essential feature for the biological activity of these piano-stool Ru^{II} complexes or if another face-capping ligand with a low steric demand would play the same role. For this reason we synthesized a new series of half-sandwich Ru^{II} complexes similar to the organometallic compounds described above, in which the aromatic fragment is replaced by the sulfur macrocycle 1,4,7-trithiacyclononane ([9]aneS_3), while the rest of the coordination sphere is left unchanged. The capability of [9]aneS_3 to coordinate to transition metal centers (and to ruthenium in particular) as a robust, face-capping, six-electron donor ligand, in analogy to the η^6-arene and η^5-cyclopentadienyl fragments (Figure 2), is well known.[22–27]

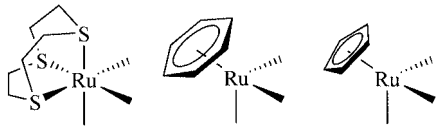

Figure 2. Schematic structural comparison of three half-sandwich Ru^{II} fragments with different face-capping ligands.

We report here the synthesis and structural characterization, both in solution and in the solid state, of the following complexes: [$RuCl_2$(PTA)([9]aneS_3)] (**4**), [RuCl(PTA)$_2$([9]aneS_3)][OTf] (OTf = triflate, $CF_3SO_3^-$) (**5**), and [RuCl(en)([9]aneS_3)][OTf] (**6**), which are analogs of some of the organometallic compounds described above; in addition, we have also prepared and characterized [RuCl(enac)([9]aneS_3)][OTf] [enac = 1,2-bis(isopropyleneimino)ethane] (**7**), [RuCl(bipy)([9]aneS_3)][OTf] (**8**), and [Ru(dmso-S)(bipy)([9]aneS_3)][OTf]$_2$ (**9**). The chemical behavior of these complexes in aqueous solution and at physiological pH have been investigated, and the in vitro tumor cell growth inhibition effects of **4**–**6** assessed.

Results and Discussion

The Precursors

Precursors for the new piano-stool compounds described below were the Ru-[9]aneS_3-dmso complexes [$RuCl_2$(dmso-S)([9]aneS_3)] (**1**), [RuCl(dmso-S)$_2$([9]aneS_3)][OTf] (**2**), and [Ru(dmso)$_3$([9]anoS_3)][OTf]$_2$ (**3**; Figure 3), in which the sulfoxides are quite easily replaced by stronger ligands. Compound **1** was first described by Landgrafe and Sheldrick in 1994,[24a] while **2** and **3** were more recently prepared by us by treatment of **1** with one or two equivalents of AgOTf, respectively.[28] Complex **3** crystallizes as [Ru(dmso-O)(dmso-S)$_2$([9]anoS_3)][OTf]$_2$ but in noncoordinating solvents it rapidly equilibrates with its linkage isomer [Ru(dmso-O)$_2$(dmso-S)([9]aneS_3)][OTf]$_2$, which is slightly more stable. Incidentally, complex **2** closely resembles the disulfoxide complex [RuCl(BESE)(η^6-*p*-cymene)][PF_6], for which James and co-workers had reported in vitro anti-cancer activity,[16] with [9]aneS_3 in place of *p*-cymene and two

S-bonded dmso's in place of the doubly S-bonded disulfoxide $EtS(O)(CH_2)_2S(O)Et$ (BESE).

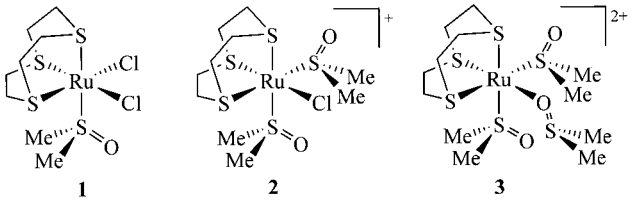

Figure 3. Schematic drawings of the precursors **1**–**3**.

All the products described below were characterized by elemental analysis, spectroscopic techniques in solution (NMR and UV/Vis spectroscopy), and in the solid state by IR spectroscopy and by X-ray diffraction analysis.

PTA Compounds

The reaction of **1** with one equivalent of 1,3,5-triaza-7-phosphaadamantane (PTA) in refluxing nitromethane led, upon selective replacement of dmso, to the isolation of the neutral compound $[RuCl_2(PTA)([9]aneS_3)]$ (**4**) in high yield (Scheme 1).

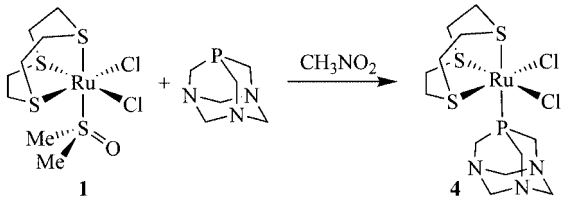

Scheme 1.

The ^1H NMR spectrum of **4** in D_2O (the only solvent in which the complex is highly soluble), recorded immediately after dissolution, shows a manifold of partially overlapping multiplets (δ = 2.6–3.0 ppm) attributed to the CH_2 protons of the [9]aneS_3 ligand,[29] and two equally intense signals (narrow unresolved multiplets) for the PTA ligand (δ = 4.22 and 4.55 ppm). By comparison with the spectrum of $[RuCl_2(PTA)(\eta^6\text{-}p\text{-cymene})]$,[12a] the downfield singlet was assigned to the CH_2 protons in the nitrogen heterocycle of PTA and the other to the CH_2 protons in the phosphorus-nitrogen heterocycle of PTA. The ^{31}P NMR spectrum shows a singlet at δ = –33.41 ppm {cf. δ = –36.63 ppm for $[RuCl_2(PTA)(\eta^6\text{-}p\text{-cymene})]$ in $CDCl_3$}.

In the solid state, the metal exhibits the expected distorted octahedral geometry (Figure 4). The Ru–ligand bond lengths are slightly different in the two independent molecules (A and B) identified in the asymmetric unit. The Ru–P bond lengths [2.290(3) Å and 2.279(2) Å] are similar to those observed in $[RuCl_2(PTA)(\eta^6\text{-}p\text{-cymene})]$.[12a] The Ru–Cl distances fall in a range from 2.429(3) to 2.459(3) Å and are similar to those in the precursor **1**.[24a] The three Ru–S bond lengths are remarkably different: those *trans* to Cl are significantly shorter [2.233(3)–2.275(3) Å, similar to those in precursors **1**] than that *trans* to the PTA phosphorus donor [2.365(3) and 2.349(3) Å in A and B, respectively]. The latter are comparable to the Ru–S bond length *trans* to phosphorus found in $[RuCl_2(PPh_3)([9]aneS_3)]$ [2.356(2) Å].[30] Water molecules (two for each complex unit) occupy voids in the crystal lattice and interact through H-bonds with the chloride ligands and with the PTA nitrogens.

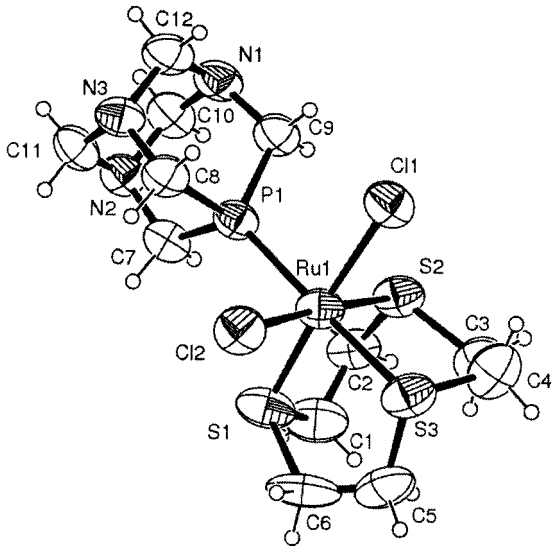

Figure 4. X-ray molecular structure of one of the two independent complexes of $[RuCl_2(PTA)([9]aneS_3)]\cdot 2(H_2O)$ (**4**). Selected bond lengths [Å] and angles [°], with data in parentheses referring to the second unit: Ru(1)–S(1) 2.248(3) [2.233(3)], Ru(1)–S(2) 2.275(3) [2.261(3)], Ru(1)–S(3) 2.365(3) [2.349(3)], Ru(1)–Cl(1) 2.429(3) [2.445(3)], Ru(1)–Cl(2) 2.429(3) [2.459(3)], Ru(1)–P(1) 2.290(3) [2.279(2)]; P(1)–Ru(1)–S(3) 175.2(1) [175.4(1)], S(1)–Ru(1)–Cl(1) 175.7(1) [174.5(1)], S(2)–Ru(1)–Cl(2) 175.5(1) [177.1(1)].

Treatment of $[RuCl(dmso)_2([9]aneS_3)][OTf]$ (**2**) with two equivalents of PTA in refluxing methanol yielded the cationic compound $[RuCl(PTA)_2([9]aneS_3)][OTf]$ (**5**) (Scheme 2).

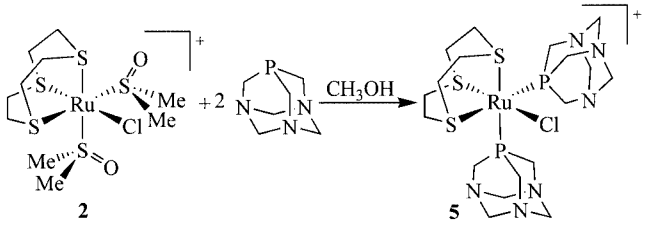

Scheme 2.

The ^1H NMR spectrum of **5** in D_2O is similar to that of **4**: the two equivalent PTA ligands give two resonances, integrating for 12 protons each, at δ = 4.25 and 4.59 ppm. The ^{31}P NMR spectrum shows a single resonance at δ = –33.45 ppm for the two equivalent phosphorus atoms. In the solid state (Figure 5), the two Ru–P bond lengths [2.317(2) and 2.315(2) Å] and the Ru–Cl distance [2.442(2) Å] present a trend similar to that found in the crystal of **4**, with values comparable to those found in

$[RuCl(PTA)_2(\eta^5\text{-}C_5Me_5)]$.[17] As previously observed (complex **4**), the Ru–S bond length *trans* to Cl [2.295(2) Å] is shorter than those *trans* to the PTA ligands [2.395(2) and 2.372(2) Å].

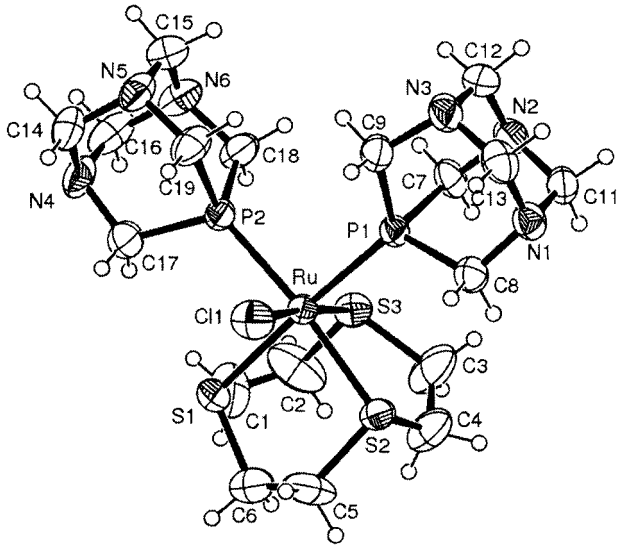

Figure 5. X-ray molecular structure of the complex cation of $[RuCl(PTA)_2([9]aneS_3)][OTf]\cdot(CH_3OH)$ (**5**). Selected bond lengths [Å] and angles [°]: Ru–S(1) 2.395(2), Ru–S(2) 2.372(2), Ru–S(3) 2.295(2), Ru–Cl(1) 2.442(2), Ru–P(1) 2.317(2), Ru–P(2) 2.315(2); P(1)–Ru–S(1) 176.66(7), P(2)–Ru–S(2) 174.17(7), S(3)–Ru–Cl(1) 174.68(7).

Ethylenediamine Compounds

The reaction of $[RuCl(dmso\text{-}S)_2([9]aneS_3)][OTf]$ (**2**) with one equivalent of ethylenediamine in refluxing nitromethane yielded, upon replacement of the two dmso ligands, the cationic compound $[RuCl(en)([9]aneS_3)][OTf]$ (**6**) (Scheme 3).

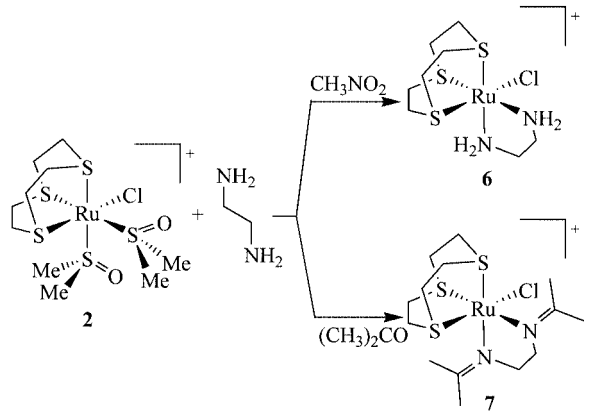

Scheme 3.

According to the X-ray structural analysis (Figure 6), the Ru–N and Ru–Cl bond lengths, as well as the chelating N–Ru–N angle, are comparable with the values found by Sadler and co-workers for the $[RuCl(en)(\eta^6\text{-arene})][PF_6]$ compounds.[10] The Ru–S distance *trans* to Cl [2.256(1) Å] is similar to the shortest one in **4**, and those *trans* to the N atoms agree with values documented for [9]aneS$_3$ *trans* to nitrogen ligands.[24a,25,28]

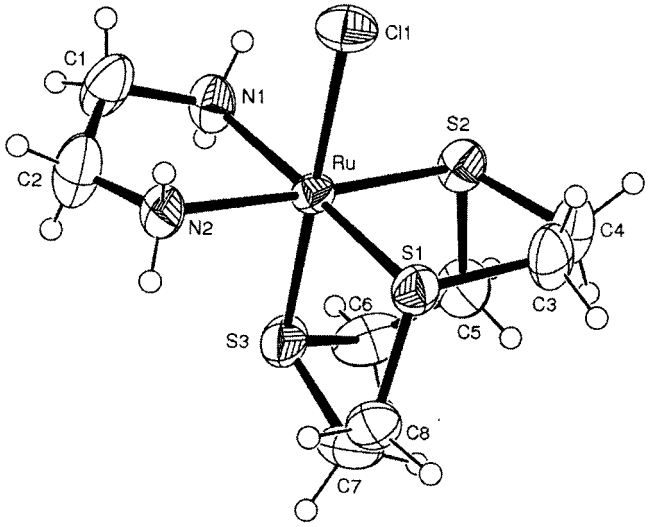

Figure 6. X-ray molecular structure of the complex cation of $[RuCl(en)([9]aneS_3)][OTf]$ (**6**). Selected bond lengths [Å] and angles [°]: Ru–S(1) 2.268(3), Ru–S(2) 2.290(3), Ru–S(3) 2.256(1), Ru–Cl(1) 2.443(1), Ru–N(1) 2.119(9), Ru–N(2) 2.180(7); N(1)–Ru–N(2) 80.7(1), N(1)–Ru–S(1) 175.4(2), N(2)–Ru–S(2) 176.3(3), S(3)–Ru–Cl(1) 179.7(1).

The $^{13}C\{^1H\}$ NMR spectrum of **6** in CD_3NO_2 (three resonances for the six CH_2 groups of [9]aneS$_3$ and a single resonance for the two CH_2 groups of the en ring) shows that the symmetry of the complex in solution (C_s) is higher than that observed in the solid state. Owing to rapid conformational equilibration of the [9]aneS$_3$ and en ligands, the complex has a plane of symmetry in solution that contains the S–Ru–Cl axis and bisects the [9]aneS$_3$ and the opposite en ligand. The ^1H NMR spectrum of **6** in CD_3NO_2 shows, besides the multiplets for [9]aneS$_3$, four equally intense, well-resolved signals for the coordinated ethylenediamine (Supporting Information). In accordance with the C_s symmetry {and by comparison with the assignements of $[RuCl(en)(\eta^6\text{-arene})]^+$ compounds}, the relatively broad resonances at δ = 3.35 and 3.91 ppm (coupled in the H-H COSY spectrum) were assigned to the two pairs of diastereotopic protons on the equivalent NH_2 groups, while the multiplets at δ = 2.83 and 2.94 ppm (coupled in the H-H COSY spectrum) were assigned to the two pairs of diastereotopic protons on the CH_2 groups. These latter resonances are coupled to the CH_2 signal of en at δ = 45.9 ppm in the H-C COSY spectrum. The ^1H NMR spectrum in D_2O is similar, but the two CH_2 resonances overlap with the multiplets of [9]aneS$_3$ (see below).

When the reaction between **2** and ethylenediamine was performed in refluxing acetone, condensation between the ligand and the solvent occurred to give 1,2-bis(isopropyleneimino)ethane (enac), which binds to ruthenium as a chelate. The cationic species $[RuCl(enac)([9]aneS_3)][OTf]$ (**7**) was thus obtained in good yield as a yellow solid and the structure was confirmed by X-ray analysis (Figure 7).

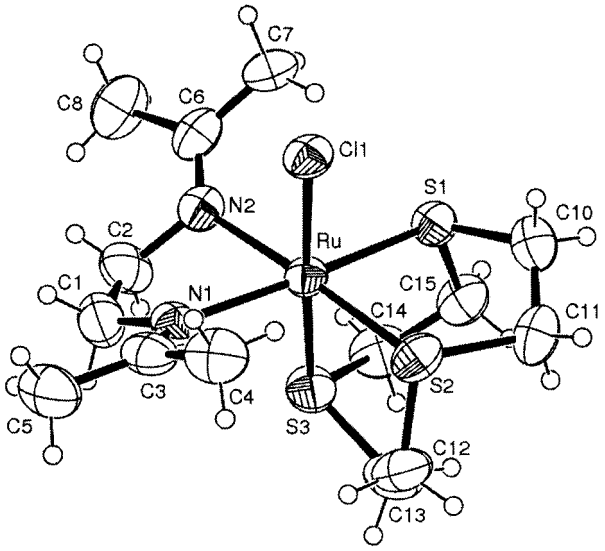

Figure 7. X-ray molecular structure of the complex cation of [RuCl(enac)([9]aneS_3)][OTf]·0.75H_2O (**7**). Selected bond lengths [Å] and angles [°]: Ru–S(1) 2.378(2), Ru–S(2) 2.414(2), Ru–S(3) 2.132(2), Ru–Cl(1) 2.296(2), Ru–N(1) 2.220(6), Ru–N(2) 2.239(5); N(1)–Ru–N(2) 74.3(2), N(1)–Ru–S(1) 173.4(1), N(2)–Ru–S(2) 177.4(1), S(3)–Ru–Cl(1) 176.26(7).

Complex **7** exhibits geometrical features that are remarkably different to the other structures reported and to those expected for similar Ru species. In fact, the Ru–N bond lengths are significantly longer than those found in compound **6** with the en ligand [2.220(6) and 2.239(5) Å vs. 2.119(9) and 2.180(7) Å]. In addition, the two Ru–S bond lengths *trans* to N [2.3776(18), 2.4139(18) Å] are extremely long if compared with those in **6**. Conversely, the Ru–Cl and the *trans* Ru–S bonds are exceptionally short: 2.296(2) and 2.132(2) Å, respectively [the Ru–Cl distance has to be compared with the value of 2.443(1) Å found in **6**]. These features can be ascribed to the steric requirements of the chelating N ligand that presents a bowed arrangement with coplanar N=C$(Me)_2$ groups that make an angle of 43.8(3)°. Methyls C(4) and C(7) point towards the chloride at a distance of around 3.54 Å.

The ^{1}H NMR spectrum of **7** in CD_3NO_2 shows, besides the [9]aneS_3 resonances, an unresolved multiplet at δ = 3.90 ppm for the four CH_2 protons and two singlets (6 H each) at δ = 2.23 and 2.57 ppm for the two pairs of diastereotopic methyl groups of the 1,2-bis(isopropyleneimino)-ethane ligand.

2,2′-Bipyridine Compounds

The reaction between [RuCl(dmso-S)$_2$([9]aneS_3)][OTf] and one equivalent of 2,2′-bipyridine (bipy) in refluxing methanol led again to the selective replacement of the two sulfoxides and formation of the cationic compound [RuCl(bipy)([9]aneS_3)][OTf] (**8**) (Scheme 4). The analogous complex [RuCl(bipy)([9]aneS_3)]Cl, as the chloride salt, has been prepared (and structurally characterized) by Goodfellow and co-workers upon reaction of **1** with a slight excess of bipy in refluxing ethanol.[26a]

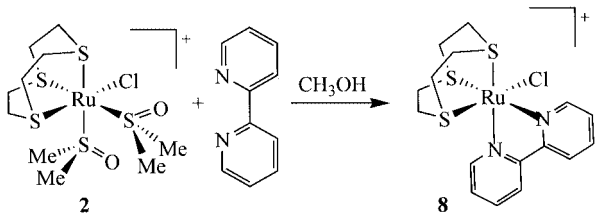

Scheme 4.

The geometry of the product was confirmed by X-ray crystallography (Figure 8). The Ru–N [2.094(4) and 2.102(4) Å], Ru–Cl [2.426(1) Å], and Ru–S [2.280(1) Å *trans* to Cl; 2.298(1) (Å) *trans* to N] bond lengths are consistent with those previously reported for the chloride derivative.[26a]

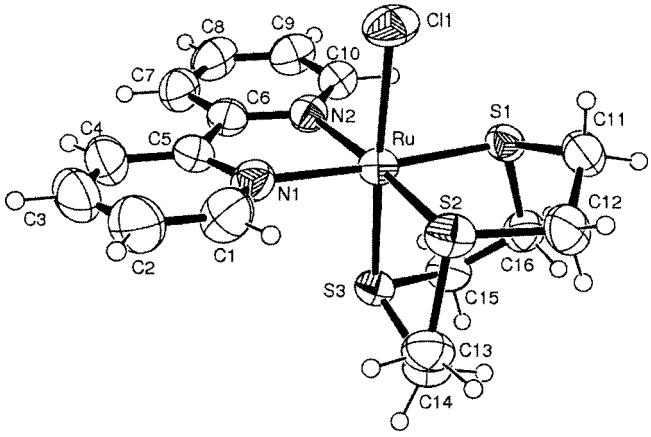

Figure 8. X-ray molecular structure of the complex cation of [RuCl(bipy)([9]aneS_3)][OTf] (**8**). Selected bond lengths [Å] and angles [°]: Ru–S(1) 2.298(1), Ru–S(2) 2.299(1), Ru–S(3) 2.280(1), Ru–Cl(1) 2.426(1), Ru–N(1) 2.102(4), Ru–N(2) 2.094(4); N(2)–Ru–N(1) 77.9(2), N(1)–Ru–S(1) 175.6(1), N(2)–Ru–S(2) 174.5(1), S(3)–Ru–Cl(1) 176.12(5).

The ^{1}H NMR spectrum of **8** in CD_3NO_2 shows four equally intense signals in the aromatic region for the coordinated bipy, indicating that the two halves of the chelate are equivalent.

Similarly, [Ru(dmso-S)(bipy)([9]aneS_3)][OTf]$_2$ (**9**), in which the chloride of **8** is formally replaced by a dmso-S ligand, was obtained by treatment of the dicationic precursor [Ru(dmso)$_3$([9]aneS_3)][OTf]$_2$ (**3**) with one equivalent of 2,2′-bipyridine in refluxing methanol (Scheme 5). The X-ray structure of **9** is shown in Figure 9. The coordination bond lengths and angles are in agreement with the parameters found in **8**, but the Ru–S(3) bond length *trans* to dmso is slightly longer than the corresponding value *trans* to Cl in **8** [2.339(3) vs. 2.280(1) Å], thus indicating a different *trans* influence for dmso and chlorine, as previously observed.[24a] The Ru–S(dmso) bond length of 2.285(3) Å is very similar to that in the precursor **1** [2.287(2) Å]. The plane of bipy forms a dihedral angle of about 12° with the N(1), N(2), S(1), and S(2) donors, away from the axial dmso ligand.

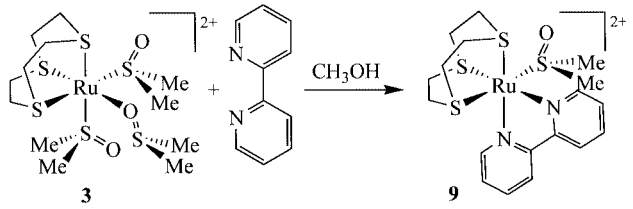

Scheme 5.

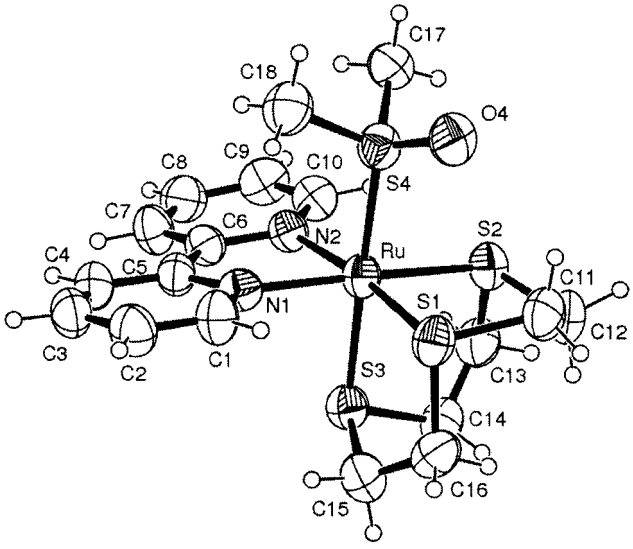

Figure 9. X-ray molecular structure of the complex cation of $[Ru(dmso\text{-}S)(bipy)([9]aneS_3)][OTf]_2{\cdot}2(H_2O)$ (**9**). Selected bond lengths [Å] and angles [°]: Ru–S(1) 2.322(3), Ru–S(2) 2.311(2), Ru–S(3) 2.339(3), Ru–S(4) 2.285(3), Ru–N(1) 2.071(7), Ru–N(2) 2.100(7); N(1)–Ru–N(2) 77.8(3), N(1)–Ru–S(2) 174.0(2), N(2)–Ru–S(1) 173.1(2), S(4)–Ru–S(3) 178.48(9).

The ^{1}H NMR spectrum of **9** in D_2O is similar to that of **8**, with an additional singlet at δ = 2.83 for the equivalent methyl groups of the dmso-S ligand. This resonance is remarkably upfield-shifted for a dmso coordinated through S, and actually falls in the region typical for dmso-O, because of the shielding cone of the adjacent bipy, as becomes apparent from the X-ray structure (Figure 9). The S=O stretching vibration in the solid state falls at an unusually high energy (1160 cm^{-1}), suggesting that in this dicationic complex dmso-S acts mainly as a σ-donor.

Llobet et al. have stated that $[9]aneS_3$ exerts a strong steric interaction on the *cis* ligands on the basis that in $[Ru(H_2O)(phen)([9]aneS_3)][ClO_4]_2$ the *cis* X–Ru–S angles are larger than 90°.[27b] However, in all structures reported the S–Ru–S angles involving the $[9]aneS_3$ are in a range from 82.68(7) to 89.6(1)°, and these values are likely to be dependent on the nature of the macrocycle. A careful inspection of the *cis* X–Ru–S bond angles reveals that these are larger than 90° in **4** and **5** (X = P), due to the bulk of the PTA ligand, and in **6**–**9** (X = N) because of the small bite angle of the chelating nitrogen ligand. Thus, these slight deformations are not ascribable to the bulk of the $[9]aneS_3$ ligand but, rather, to the geometrical requirements of the other ligands, as confirmed by the fact that the *cis* Cl–Ru–S bond angles are close to, or slightly less than, 90°.

As a conclusion it is worthwhile to note that X-ray diffraction studies indicate close geometrical similarities between the present complexes and the piano-stool Ru^{II} compounds bearing an η^6-arene ligand instead of the $[9]aneS_3$ tripodal group.

Chemical Behavior in Aqueous Solution

These new piano-stool ruthenium complexes were prepared with the aim of comparing their biological activities with those of the corresponding organometallic compounds bearing an aromatic fragment in place of the $[9]aneS_3$ ligand. Thus, as a first step, the chemical behavior of compounds **4**–**9** was investigated in water, in the presence of 100 mM NaCl (that mimics the extracellular chloride concentration), and in PBS buffer solution at physiological pH (0.01 M phosphate buffer, pH 7.4, 0.9% NaCl) by ^{1}H NMR and UV/Vis spectroscopy.

Both the ^{1}H NMR and UV/Vis spectra of the neutral PTA complex $[RuCl_2(PTA)([9]aneS_3)]$ (**4**) changed quite rapidly during the first 30 min after dissolution in water due to dissociation of one chloride to give $[RuCl(H_2O)(PTA)([9]aneS_3)]^+$ (**4a**). The evolution of the absorption spectrum is characterized by two isosbestic points at 330 and 408 nm (Supporting Information). In the ^{1}H NMR spectrum the two PTA resonances of **4** (δ = 4.22, 4.55 ppm) are gradually replaced by those of **4a** (δ = 4.23, 4.57 ppm), which are only slightly shifted downfield; no signals for the free ligands were observed.[31] The spectra remained unchanged afterwards, even after prolonged periods (weeks), indicating that **4a** is stable. Addition of 100 mM NaCl to a D_2O solution of **4a** reversed the hydrolytic process completely, and the original NMR spectrum of **4** was immediately re-obtained (Supporting Information). A pK_a value of 3.3 for coordinated PTA in **4a** was obtained from a ^{31}P NMR pH titration curve in D_2O (Supporting Information). For comparison, a pK_a value of 3.13 has been estimated from a ^{31}P NMR titration for coordinated PTA in the $[RuCl_2(PTA)(\eta^6\text{-}p\text{-cymene})]$ complex,[14] while a pK_a value of 10.1 was similarly obtained for the coordinated water molecule in $[Ru(H_2O)(phen)([9]aneS_3)]^{2+}$.[27b] Conversely, the p$K_a$ values of the coordinated water in $[Ru(H_2O)(en)(\eta^6\text{-arene})]^{2+}$ adducts, as determined by ^{1}H NMR spectroscopy, are in the range 7.71–8.25.[32]

In phosphate buffered saline (pH 7.4) the hydrolysis of **4** to **4a** occurs as in water, but is followed by a further slow reaction leading to a new species **4b**. In the ^{1}H NMR spectrum this process is accompanied by the gradual decrease of the two PTA resonances of **4a** and simultaneous growth of two new signals (δ = 4.28 and 4.60 ppm) for **4b**. After 15 days at ambient temperature **4a** and **4b** are present in solution in approximately equal amounts. This slow process is perhaps due to partial dissociation of the chloride of **4a** to yield $[Ru(H_2O)_2(PTA)([9]aneS_3)]^{2+}$ (**4b**); however, coordination of phosphate, as observed in the $[Ru(H_2O)(en)(\eta^6\text{-ar-}$

ene)]$^{2+}$ and [Ru(H_2O)Cl(PTA)(η^6-arene)]$^+$ species,[14,32] cannot be excluded (see below).

The cationic PTA complex [RuCl(PTA)$_2$([9]$aneS_3$)][OTf] (**5**) was found to be remarkably inert both in water and at physiological pH. No significant spectral changes were observed over a period of two weeks. Addition of 100 mM Cl induced no spectral changes (Supporting Information). A pK_a value of 2.4 for coordinated PTA in **5** was obtained from a ^{31}P NMR pH titration curve in D_2O (Supporting Information).

Investigation of the behavior of [RuCl(en)([9]$aneS_3$)][OTf] (**6**) in aqueous solution by ^{1}H NMR spectroscopy is difficult due to overlap of the signals of the CH_2 protons of en and [9]$aneS_3$. In the ^{1}H NMR spectrum of **6** in D_2O immediately after dissolution two sets of NH_2 signals, belonging to two species in an approximate 3:1 ratio, are observed (Supporting Information). The spectrum remained basically unchanged for days. Addition of 100 mM NaCl reversed the initial ratio between the two sets of NH_2 resonances immediately, suggesting the presence of an equilibrium between the two species (Supporting Information). Thus, the resonances of the most intense set (δ = 3.87, 4.70 ppm) were assigned to the aquated species [Ru(H_2O)(en)([9]$aneS_3$)]$^{2+}$ (**6a**), while those of the minor set (δ = 3.65, 4.54 ppm) were attributed to the parent compound **6**, which becomes predominant in the presence of excess chloride. The ^{1}H NMR spectrum in buffer solution, besides the NH_2 signals of **6** and **6a**, shows two other less-intense broad resonances at δ = 4.35 and 4.45 ppm, assigned to the NH_2 of coordinated en in a new species **6b**. The signals of **6** decrease slowly with time while those of **6a** and **6b** correspondingly increase, and after one week **6b** was the main species in solution. Tentatively, **6b** might form from **6a** upon phosphate coordination (no signals for free ethylendiamine or [9]$aneS_3$ were observed to grow with time).

The ^{1}H NMR spectrum of [RuCl(enac)([9]$aneS_3$)][OTf] (**7**) in D_2O recorded immediately after dissolution is similar to that in CD_3NO_2 (see above) and remains unchanged with time. However, upon addition of NaCl the resonances of a new species, of almost equal intensity, appear immediately beside those of the original species (Supporting Information). Thus, the resonances of the original set were assigned to the aquated species [Ru(H_2O)(enac)([9]$aneS_3$)]$^{2+}$ (**7a**; for example, the singlets of the methyl groups appear at δ = 2.23 and 2.57 ppm), while those of the new set (methyl groups at δ = 2.22 and 2.61 ppm) were attributed to the parent compound **7**, which is in equilibrium with **7a**. In the absence of free chloride, this equilibrium is completely shifted towards **7a** at NMR concentrations. The ^{1}H NMR spectrum in phosphate-buffered saline solution shows, besides the signals of **7** and **7a**, the resonances of yet another species with coordinated enac, **7b**, which were found to grow slowly with time (days). No signals for the free ligands were observed during these processes. Most likely, also in this case **7b** is derived from **7a** upon coordination of phosphate.

[RuCl(bipy)([9]$aneS_3$)][OTf] (**8**) is relatively labile in aqueous solution. The ^{1}H NMR spectrum recorded immediately after dissolution of the complex in D_2O shows two sets of signals for the coordinated bipy in an approximate 3:2 ratio (Supporting Information). The most abundant set was assigned to **8** and the other, which grows with time, to the dicationic aquated species [Ru(H_2O)(bipy)([9]$aneS_3$)]$^{2+}$ (**8a**).[33] After 30 min the ratio between **8** and **8a** was about 1:2 (Supporting Information), and the equilibrium could be reversed by the addition of chloride. During the hydrolytic process, no signals for free bipy or [9]$aneS_3$ were observed. The same aquo species **8a** was obtained, but much more slowly (days), from [Ru(dmso-S)(bipy)([9]$aneS_3$)][OTf]$_2$ (**9**) upon dissociation of the dmso ligand (Scheme 6). In this case the process could also be followed by monitoring the growth of the resonance of free dmso at δ = 2.72 ppm.

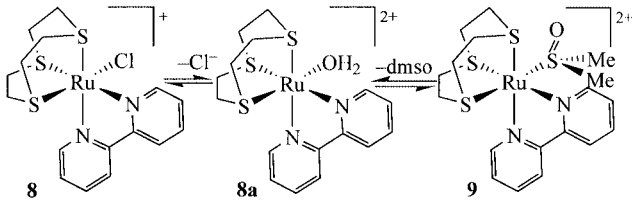

Scheme 6.

The behavior of **8** and **9** at pH 7.4 is similar to that found in water and is mainly influenced by the presence of free chloride in the buffer. Thus, for both complexes the equilibrium amount of **8a** is lower than in pure water and compound **9** slowly equilibrates also with **8** (Scheme 6). In addition, for both complexes the signals of a new species with coordinated bipy, presumably with phosphate bound in the place of water, were observed to grow slowly with time.

Cell Growth Inhibition Effects on TS/A Adenocarcinoma Cells and on HBL-100 Mammary Cells

The MTT test, which measures mitochondrial dehydrogenase activity as an indication of cell viability, was carried out with the water-soluble compounds [$RuCl_2$(PTA)([9]$aneS_3$)] (**4**), [RuCl(PTA)$_2$([9]$aneS_3$)][OTf] (**5**), and [RuCl(en)([9]$aneS_3$)][OTf] (**6**) using two different cell lines − tumour mouse TS/A cells and normal human HBL-100 cells. The effects of compounds **4**–**6** on the cell growth were evaluated after treatment for 24, 48, and 72 h. The cell viability after these times was determined by the MTT assay and the results from these studies are summarized in Figure 10. The experiments were performed in quadruplicate and repeated twice for all three compounds; the IC_{50} values resulting from an average over the two experiments are listed in Table 1.

Compounds **4**–**6** show different in vitro behaviors against the mouse adenocarcinoma cancer cell line (TS/A) and against the human mammary nontumor cell line (HBL-100). Complex **4** is scarcely cytotoxic and shows IC_{50} values that are high and very similar in both cell lines. It is worth comparing these data with the aromatic [$RuCl_2$(PTA)(η^6-arene)] analogs of complex **4**, values for which are also given in Table 1.

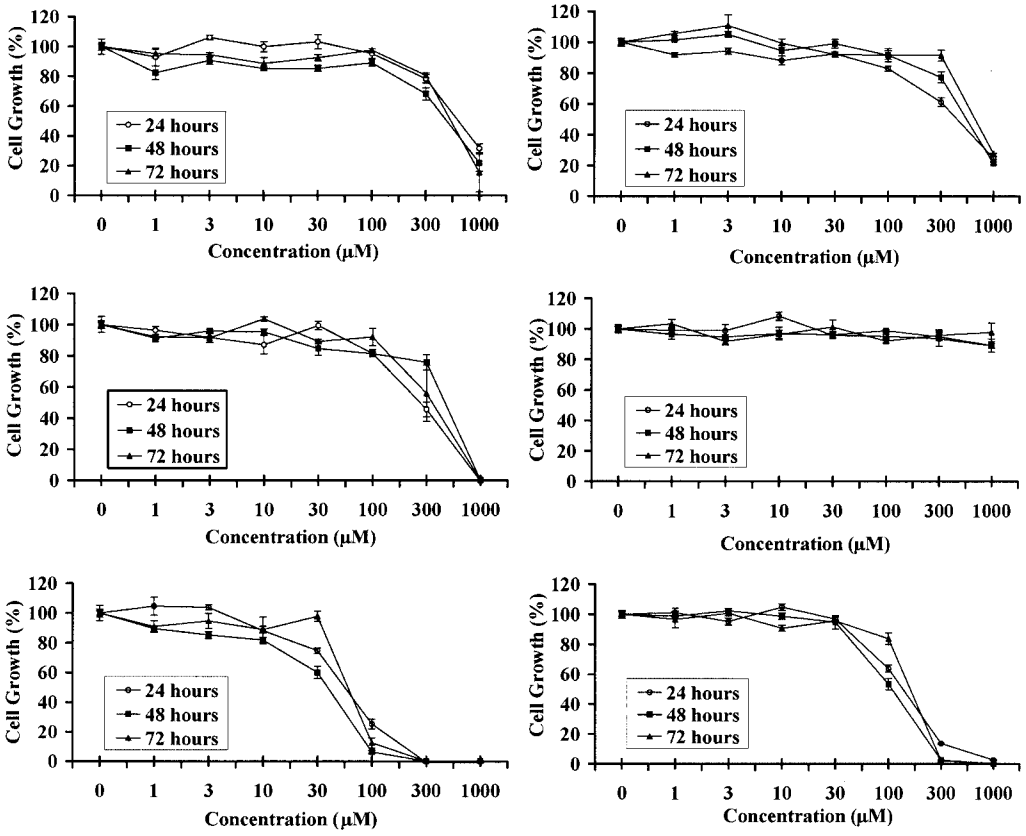

Figure 10. Effects of [$RuCl_2$(PTA)([9]$aneS_3$)] (**4**) (top), [RuCl(PTA)$_2$([9]$aneS_3$)][OTf] (**5**) (middle), and [RuCl(en)([9]$aneS_3$)][OTf] (**6**) (bottom) on TS/A (left) and HBL-100 (right) cell proliferation. The cells were sown on day 0 and treated on day 1 with a range of concentrations between 1–1000 μM of compounds **4**–**6** for 24, 48, and 72 hours. Cell growth was evaluated using the MTT test at the end of the treatment.

Table 1. IC_{50} values of [$RuCl_2$(PTA)([9]$aneS_3$)] (**4**), [RuCl(PTA)$_2$([9]$aneS_3$)][OTf], (**5**) and [RuCl(en)([9]$aneS_3$)][OTf], (**6**) on the TS/A and HBL-100 cell lines after incubation for 72 h.

Compound	IC_{50} (TS/A) [μM]	IC_{50} (HBL-100) [μM]
[$RuCl_2$(PTA)([9]$aneS_3$)] (**4**)	650	738
[RuCl(PTA)$_2$([9]$aneS_3$)][OTf] (**5**)	388	>1000
[RuCl(en)([9]$aneS_3$)][OTf] (**6**)	65	175
[$RuCl_2$(PTA)(η^6-*p*-cymene)][a]	507	>1000
[$RuCl_2$(PTA)(η^6-benzene)][a]	231	>1000

[a] IC_{50} values taken from ref. 14.

A larger difference in cytotoxicity between the two cell lines is observed for complex **5**, which is mildly active against the TS/A adenocarcinoma cells with an IC_{50} value of 388 μM after 72 h of incubation, but is essentially nontoxic to the HBL-100 normal cells under analogous conditions, even at very high concentrations (IC_{50} > 1000 μM). It thus appears that the presence of two PTA ligands is important to have a selectivity of the compounds towards the cancer cells.

Complex **6** is the most cytotoxic among those tested and it is also somewhat selective towards cancer cells (Table 1). The aromatic analogs of complex **6**, developed by Sadler and co-workers,[8,9] also show greater cytotoxicity than Ru^{II}–arene PTA complexes (aromatic analogs of complex **4**).[14] A direct comparison between **6** and the corresponding [RuCl(en)(η^6-arene)][PF_6] complexes is difficult as cytotoxicity tests were performed against different cell lines; for example, [RuCl(en)(η^6-*p*-cymene)][PF_6] has an IC_{50} value of 10 μM against A2780 cells. Nevertheless, from these data it appears that the aromatic fragment is not essential for cytotoxicity and that the [9]$aneS_3$ ligand can be used in its place.

Conclusions

In summary, some new half-sandwich Ru^{II}-[9]$aneS_3$ complexes, namely [$RuCl_2$(PTA)([9]$aneS_3$)] (**4**), [RuCl(PTA)$_2$([9]$aneS_3$)][OTf] (**5**), [RuCl(en)([9]$aneS_3$)][OTf] (**6**), [RuCl(enac)([9]$aneS_3$)][OTf] (**7**), [RuCl(bipy)([9]$aneS_3$)][OTf] (**8**), and [Ru(dmso-S)(bipy)([9]$aneS_3$)][OTf]$_2$ (**9**) have been prepared from Ru-[9]$aneS_3$-dmso precursors and structurally characterized. Some of them are analogs of known cytotoxic organometallic Ru^{II}-(η^6-arene) and Ru^{II}-(η^5-cyclopentadienyl) compounds, in which the aromatic fragment is replaced by the sulfur macrocycle 1,4,7-trithiacyclononane while the rest of the coordination sphere is left unchanged.

For all new complexes, the results from the X-ray studies are consistent with the NMR spectroscopic data, thus indi-

cating that the structures observed in the solid state are maintained in solution. Owing to rapid conformational equilibration of the [9]aneS_3 (and en ligand in **6**), the symmetry of each complex in solution (C_s) is higher than in the solid state. In solution they have a plane of symmetry that contains the S–Ru–X axis (X = P in **4**; X = Cl in **5**–**8**; X = S in **9**) and bisects the [9]aneS_3 and the opposite ligands (either two equal monodentate ligands as in **4** and **5**, or a chelate as in **6**–**9**). Similarly to the aromatic analogs for which data are available, in aqueous solution the Ru-[9]-aneS_3 complexes (with the exception of **5**) hydrolyze a chloride (or a dmso in the case of **9**) to give the corresponding aquo species. This process is rapidly reversed in the presence of free chloride, and coordination of phosphate to the aquo species is likely to occur in phosphate-buffered solutions at physiological pH. No dissociation of [9]aneS_3 or of the other ligands was observed.

Preliminary in vitro tests were performed on three complexes (**4**–**6**) against the mouse adenocarcinoma cancer cell line (TS/A) and the human mammary normal cell line (HBL-100). In general, the Ru-[9]aneS_3 compounds have a cytotoxicity comparable to that of the corresponding organometallic analogs. The most cytotoxic complex among those tested was [RuCl(en)([9]aneS_3)][OTf] (**6**), with IC_{50} values of 65 μM (TS/A) and 175 μM (HBL-100). Most interestingly, compounds **5** and **6** are more cytotoxic against the cancer cell line (TS/A) than against the human mammary normal cell line (HBL-100); thus, they might lead to anticancer activity with low general toxicity and hence low side-effects.

In conclusion, the results of the in vitro studies suggest that the aromatic fragment of the piano-stool Ru^{II} compounds is not an essential feature for the in vitro anticancer activity, and it might be effectively replaced by another face-capping ligand with a low steric demand such as [9]-aneS_3. As Sadler and co-workers have shown that there is a direct correlation between cytotoxicity and the size (and therefore the lipophilicity) of the arene, it is possible that in the future the cytotoxicity of the Ru-[9]aneS_3 complexes might similarly be increased by using more lipophilic ligands.

Experimental Section

UV/Vis spectra were obtained on a Jasco V-550 spectrometer in quartz cells. ^1H and ^{13}C NMR spectra were recorded at room temperature at 400 and 100.5 MHz, respectively, on a JEOL Eclipse 400 FT instrument. All spectra were recorded at room temperature. Proton peak positions were referenced to 2,2-dimethyl-2,2-silapentane-5-sulfonate (DSS, set at δ = 0.00 ppm) in D_2O, or to the peak of residual non-deuterated solvent set at δ = 4.33 ppm in CD_3NO_2. Carbon peak positions were referenced to DSS (set at δ = 0.0 ppm) in D_2O, or to the central peak of the solvent set at δ = 62.8 ppm in CD_3NO_2. ^{31}P NMR spectra were recorded on a Bruker Avance DPX 400 MHz spectrometer at 161.9 MHz. Infrared spectra (KBr) were recorded on a Perkin–Elmer 983G spectrometer or on a Perkin–Elmer 2000 NIR FT-Raman spectrometer. ESI mass spectra of the complexes were obtained on a Thermofinigan LCQ Deca XP Plus quadrupole ion trap instrument set in positive mode (solvent: methanol; flow rate: 5 μL min^{-1}; spray voltage: 5 kV; capillary temperature: 100 °C; capillary voltage: 20 V), as described previously.[34] Elemental analysis (C, H, N) was performed at the Dipartimento di Scienze Chimiche, Università di Trieste. [$RuCl_2$(dmso-S)([9]aneS_3)] (**1**),[24] [RuCl(dmso-S)$_2$([9]aneS_3)][OTf] (**2**),[28] [Ru(dmso)$_3$([9]anoS_3)][OTf]$_2$ (**3**),[28] and PTA[35] were prepared according to literature procedures. Trithiacyclononane was purchased from Aldrich.

The pH titration curves, reporting the chemical shift of the ^{31}P NMR spectra vs. the pD values, were fitted to the Henderson–Hasselbalch equation using the program Micromath® Scientist® with the assumption that the observed chemical shifts are weighted averages according to the populations of the protonated and deprotonated species. The resonance frequencies change smoothly with pH between the chemical shifts of the charged form HA^+, and those of the neutral, deprotonated form A, which is present at high pH. At any pH, the observed chemical shift is a weighted average of the two extreme values $\delta(HA^+)$ and $\delta(A)$:

$$\delta_{av} = \frac{\delta(HA^+)[HA^+]+\delta(A)[A]}{[HA^+]+[A]}$$

The midpoint of the titration curve occurs when the concentrations of the acid and its conjugate base are equal: $[HA^+] = [A]$, i.e. when the pH equals the pK_a of the compound.

[$RuCl_2$(PTA)([9]aneS_3)] (4): PTA (37 mg, 0.16 mmol) was added to [$RuCl_2$(dmso-S)([9]aneS_3)] (**1**; 100 mg, 0.16 mmol) partially dissolved in nitromethane (15 mL). The mixture was then heated to reflux to yield a yellow solution after 2–3 min, and a yellow-orange solid after about 10 min. After 2 h reflux, the precipitate was removed by filtration, washed with cold nitromethane and diethyl ether, and vacuum dried. Yield: 51 mg (62%). $C_{12}H_{24}Cl_2N_3PRuS_3$ (509.47): calcd. C 28.3, H 4.75, N 8.25; found C 28.2, H 5.11, N 8.13. ^1H NMR (400 MHz, D_2O, 25 °C): δ = 3.00–2.60 (m, 12 H, [9]aneS_3), 4.23 (s, 6 H, PTA), 4.55 (s, 6 H, PTA) ppm. $^{31}P\{^1H\}$ NMR (161.9 MHz, D_2O, 25 °C): δ = –33.41 (s) ppm. UV/Vis (H_2O, 25 °C): λ_{max} (ε) = 317 nm (632 $M^{-1}cm^{-1}$), 362 (542), 423 (390). ES-MS (MeOH): *m*/*z* = 512 (calcd. 511) [$RuCl_2$(PTA)([9]aneS_3) + $H]^+$, 492 (calcd. 492) [RuCl(H_2O)(PTA)([9]aneS_3)]$^+$, 474 (calcd. 474) [RuCl(PTA)([9]aneS_3)]$^+$.

[$RuCl(PTA)_2$([9]aneS_3)][OTf] (5): PTA (45 mg, 0.29 mmol) was added to [RuCl(dmso-S)$_2$([9]aneS_3)][OTf] (**2**; 90 mg, 0.144 mmol) partially dissolved in methanol (15 mL) and the mixture was refluxed for 2 h. The yellow solution was then concentrated in vacuo to ca. 3 mL, and a few drops of diethyl ether were added. A yellow solid formed upon standing, which was removed by filtration, washed with cold methanol and diethyl ether, and vacuum dried. Yield: 75 mg (60%). $C_{19}H_{36}ClF_3N_6O_3P_2RuS_4$ (780.24): calcd. C 29.2, H 4.65, N 10.77; found C 29.1, H 4.29, N 10.50. ^1H NMR (400 MHz, D_2O, 25 °C): δ = 2.62 (m, 2 H, [9]aneS_3), 2.92 (m, 10 H, [9]aneS_3), 4.25 (s, 12 H, PTA), 4.59 (s, 12 H, PTA) ppm. ^1H NMR (400 MHz, CD_3CN, 25 °C): δ = 2.38 (m, 2 H, [9]aneS_3), 2.78 (m, 8 H, [9]aneS_3), 2.99 (m, 2 H, [9]aneS_3), 4.20 (s, 12 H, PTA), 4.50 (s, 12 H, PTA) ppm. $^{13}C\{^1H\}$ NMR (100.5 MHz, CD_3CN, 25 °C): δ = 32.1, 34.2, 41.2 (CH_2, [9]aneS_3), 54.2, 73.2 (CH_2, PTA), 123.7, 125.5 (CF_3, OTf) ppm. $^{31}P\{^1H\}$ NMR (161.9 MHz, D_2O, 25 °C): δ = –33.45 (s) ppm. UV/Vis (H_2O, 25 °C): λ_{max} (ε) = 357 nm (480 $M^{-1}cm^{-1}$), 296 (1000). ES-MS (MeOH): *m*/*z* = 631 (calcd. 631) [$RuCl(PTA)_2$([9]aneS_3)]$^+$.

[RuCl(en)([9]aneS_3)][OTf] (6): Ethylenediamine (10.7 μL, 0.16 mmol) was added to [RuCl(dmso-S)$_2$([9]aneS_3)][OTf] (**2**; 150 mg, 0.16 mmol) dissolved in nitromethane (10 mL) and the mixture was refluxed for 2 h. The yellow solution was concentrated

in vacuo to ca. 5 mL, filtered through paper, and a few drops of diethyl ether were added. A yellow-brown microcrystalline solid formed upon standing, which was removed by filtration, washed with cold nitromethane and diethyl ether, and vacuum dried. Yield: 110 mg (87%). $C_9H_{20}ClF_3N_2O_3RuS_4$ (526.03): calcd. C 20.5, H 3.83, N 5.32; found C 20.4, H 3.52, N 4.95. ^{1}H NMR (400 MHz, CD_3NO_2, 25 °C): δ = 2.8–2.3 (m, 12 H, [9]aneS$_3$), 2.83 (br., 2 H, en), 2.94 (br., 2 H, en), 3.35 (br., 2 H, NH), 3.91 (br., 2 H, NH) ppm. ^{13}C{^{1}H} NMR (100.5 MHz, CD_3NO_2, 25 °C): δ = 32.7, 33.1, 35.9 (CH_2, [9]aneS$_3$), 45.9 (CH_2, en), 120.8, 124.0 (CF_3, OTf) ppm. UV/Vis (H_2O, 25 °C): λ_{max} (ε) = 370 nm (490 M^{-1}cm^{-1}). Selected IR (KBr): $\tilde{\nu}$ = 3295 cm^{-1} (w, νNH$_2$), 3250 (w, νNH$_2$), 1577 (m, δNH$_2$), 1257, 1140, 1026 cm^{-1} (s, νOTf). ES-MS (MeOH): *m*/*z* = 377 (calcd. 377) [RuCl(en)([9]aneS$_3$)]$^+$.

[RuCl(enac)([9]aneS$_3$)][OTf] (7): Ethylenediamine (15 μL, 0.225 mmol) was added to [RuCl(dmso-S)$_2$([9]aneS$_3$)][OTf] (**2**; 140 mg, 0.1125 mmol) dissolved in acetone (20 mL) and the mixture was refluxed for 2 h. The yellow solution was concentrated in vacuo to ca. 5 mL and a few drops of diethyl ether were added. A yellow microcrystalline solid formed on standing, which was removed by filtration, washed with cold acetone and diethyl ether, and vacuum dried. Yield: 40 mg (59%). $C_{15}H_{28}ClF_3N_2O_3RuS_4$ (606.15): calcd. C 29.7, H 4.65, N 4.62; found C 30.4, H 4.34, N 4.47. ^{1}H NMR (400 MHz, D_2O, 25 °C): δ = 2.23 (s, 6 H, CH_3), 2.8–2.4 (m, 12 H, [9]aneS$_3$), 2.57 (s, 6 H, CH_3), 3.93 (m, 4 H, CH_2 enac) ppm. ^{1}H NMR (400 MHz, CD_3NO_2, 25 °C): δ = 2.24 (s, 6 H, CH_3), 2.8–2.4 (m, 12 H, [9]aneS$_3$), 2.69 (s, 6 H, CH_3), 3.90 (m, 4 H, CH_2 enac) ppm. UV/Vis (H_2O, 25 °C): λ_{max} (ε) = 275 nm (4300 M^{-1}cm^{-1}), 376 (580). Selected IR (KBr): $\tilde{\nu}$ = 1625 cm^{-1} (m, νC=N), 1267, 1148, 1031 (s, νOTf) cm^{-1}.

[RuCl(bipy)([9]aneS$_3$)][OTf] (8): 2,2′-Bipyridine (25 mg, 0.16 mmol) was added to [RuCl(dmso-S)$_2$([9]aneS$_3$)][OTf] (**2**; 100 mg, 0.16 mmol) partially dissolved in methanol (10 mL) and the mixture was refluxed for 1 h. After about 10 min the solution turned orange. Upon concentration in vacuo to ca. 3 mL an orange solid formed, which was removed by filtration, washed with cold methanol and diethyl ether, and vacuum dried. Yield: 65 mg (65%). $C_{17}H_{20}ClF_3N_2O_3RuS_4$ (622.11): calcd. C 32.8, H 3.24, N 4.50; found C 32.1, H 3.34, N 4.30. ^{1}H NMR (400 MHz, CD_3NO_2, 25 °C): δ = 3.1–2.5 (m, 12 H, [9]aneS$_3$), 7.63 (t, 2 H, H5,5′), 8.14 (t, 2 H, H4,4′), 8.48 (d, 2 H, H3,3′), 9.08 (d, 2 H, H6,6′) ppm. UV/Vis (H_2O, 25 °C): λ_{max} (ε) = 286 nm (13800 M^{-1}cm^{-1}), 420 (2350).

[Ru(dmso-S)(bipy)([9]aneS$_3$)][OTf]$_2$ (9): 2,2′-Bipyridine (11.4 mg, 0.073 mmol) was added to [Ru(dmso)$_3$([9]aneS$_3$)][OTf]$_2$ (**3**; 60 mg, 0.073 mmol) dissolved in methanol (15 mL) and the mixture was refluxed for 1 h. Upon concentration in vacuo to ca. 3 mL a yellow solid formed, which was removed by filtration, washed with cold methanol and diethyl ether, and vacuum dried. Yield: 50 mg (84%). $C_{20}H_{26}N_2F_6O_7S_4Ru$ (813.85): calcd. C 29.5, H 3.22, N 3.44; found C 29.2, H 3.14, N 3.30. ^{1}H NMR (400 MHz, D_2O, 25 °C): δ = 3.3–2.7 (m, 12 H, [9]aneS$_3$), 2.83 (s, 6 H dmso-S), 7.81 (t, 2 H, H5,5′), 8.31 (t, 2 H, H4,4′), 8.60 (d, 2 H, H3,3′), 9.05 (d, 2 H, H6,6′) ppm. Selected IR (KBr): $\tilde{\nu}$ = 163 cm^{-1} (s, νSO, dmso-S), 517 (m, νRuS, dmso-S), 1267, 1258, 1150, 1030 (s, νOTf) cm^{-1}. UV/Vis (H_2O, 25 °C): λ_{max} (ε) = 268 nm (16000 M^{-1}cm^{-1}), 306 (9800), 316 (13000), 344 (3220).

X-ray Crystallography: Diffraction data for all compounds were collected at room temperature on a Nonius DIP-1030H system with graphite-monochromated Mo-K_α radiation, with the exception of the data set of compound **4**, which was collected at 220(2) K with a Bruker–Nonius FR591 rotating anode (Cu-K_α) equipped with a KappaCCD detector. Cell refinement, indexing, and scaling of the data sets were performed with the programs Denzo and Scalepack.[36] The structures were solved by Patterson and Fourier analyses and refined by the full-matrix least-squares method based on F^2 with all observed reflections.[37] A Flack parameter of 0.55(7) for space group $P2_1$ in **6** indicates racemic twinning of the crystal. The ΔF maps revealed water molecules in **4** and **9** (two molecules per complex unit) and in **7** (residuals accounting for 0.75 water oxygen), and methanol (one molecule) in **5**. The hydrogen atoms were located at geometrically calculated positions except those of disordered water. The structural figures were drawn with ORTEP3 for Windows (ellipsoids at 40% probability level),[38] and all the calculations performed with the WinGX System, Ver 1.64.05.[39] Crystal data and details of structure refinements for compounds **4**–**9** are reported in Tables 2 and 3.

CCDC-265997–266002 (for **4**–**9**) contain the supplementary crystallographic data for this paper. These data can be obtained free

Table 2. Crystal data and details of structure refinement for compounds **4**–**6**.

	4·2H$_2$O	**5**·CH$_3$OH	**6**
Formula	$C_{12}H_{28}Cl_2N_3O_2PRuS_3$	$C_{20}H_{40}ClF_3N_6O_4P_2RuS_4$	$C_9H_{20}ClF_3N_2O_3RuS_4$
Formula mass	545.49	812.28	526.03
Crystal system	monoclinic	triclinic	monoclinic
Space group	$P2_1/n$	$P\bar{1}$	$P2_1$
a [Å]	19.271(4)	7.896(3)	7.975(3)
b [Å]	7.523(3)	14.354(4)	9.223(3)
c [Å]	28.721(4)	14.303(4)	12.235(4)
α [°]		103.33(2)	
β [°]	94.58(2)	99.63(2)	96.04(2)
γ [°]		91.83(3)	
V [Å^3]	4151(2)	1551.0(8)	894.9(5)
Z	8	2	2
$D_{calcd.}$ [g cm^{-3}]	1.746	1.739	1.952
μ [mm^{-1}]	12.142[a]	1.022	1.532
Reflections collected	47588	16888	11536
Reflections unique (R_{int})	6128 (0.0488)	5919 (0.0524)	4979 (0.0351)
Reflections $I > 2\sigma(I)$	3674	3476	3820
R_1	0.0644	0.0551	0.0382
wR_2 [$I > 2\sigma(I)$][b]	0.1846	0.1381	0.0953
Residuals [e Å^{-3}]	0.912, –0.524	0.934, –0.848	0.576, –0.529

[a] Copper radiation. [b] $R_1 = \Sigma||F_o| - |F_c||/\Sigma|F_o|$, $wR_2 = [\Sigma w(F_o^2 - F_c^2)^2/\Sigma w(F_o^2)^2]^{1/2}$.

Table 3. Crystal data and details of structure refinement for compounds **7**–**9**.

	7·H_2O	**8**	**9**·2(H_2O)
Formula	$C_{15}H_{29.50}ClF_3N_2O_{3.75}RuS_4$	$C_{17}H_{20}ClF_3N_2O_3RuS_4$	$C_{20}H_{30}F_6N_2O_9RuS_6$
Formula mass	619.67	622.11	849.89
Crystal system	monoclinic	monoclinic	triclinic
Space group	$P2_1/n$	$C2/c$	$P\bar{1}$
a [Å]	7.769(3)	24.811(4)	10.087(4)
b [Å]	10.722(3)	11.803(3)	12.625(3)
c [Å]	31.968(5)	16.384(3)	14.134(4)
α [°]			88.02(2)
β [°]	94.02(3)	100.39(3)	75.50(3)
γ [°]			68.76(2)
V [Å^3]	2656.3(13)	4719.3(17)	1621.1(9)
Z	4	8	2
$D_{calcd.}$ [g cm^{-3}]	1.549	1.751	1.741
μ [mm^{-1}]	1.047	1.177	0.953
Reflections collected	20925	19338	17550
Reflections unique (R_{int})	4900 (0.0359)	4518 (0.0679)	7909 (0.0675)
Reflections $I > 2\sigma(I)$	3058	2633	3414
R_1	0.0590	0.0394	0.0594
wR_2 [$I > 2\sigma(I)$][a]	0.1742	0.0893	0.1335
Residuals [e Å^{-3}]	0.825, –0.518	0.377, –0.476	0.623, –0.576

[a] $R_1 = \Sigma||F_o| - |F_c||/\Sigma|F_o|$, $wR_2 = [\Sigma w(F_o^2 - F_c^2)^2/\Sigma w(F_o^2)^2]^{1/2}$.

of charge from The Cambridge Crystallographic Data Centre via www.ccdc.cam.ac.uk/data_request/cif.

In vitro Tests: TS/A murine adenocarcinoma cell line, initially obtained from Dr. G. Forni (CNR, Centro di Immunogenetica ed Oncologia Sperimentale, Torino, Italy) belongs to the tumor cell panel of the Callerio Foundation (Trieste) and is stored in liquid nitrogen. Cells were cultured according to a standard procedure,[40] and maintained in RPMI-1640 medium (EuroClone, Wetherby, U.K.) supplemented with 10% Fetal Bovine Serum (FBS, Invitrogen, Milano, Italy), 2 mM L-glutamine (EuroClone) and 50 μg mL^{-1} gentamycin sulfate solution (EuroClone). The cell line was kept in a CO_2 incubator with 5% CO_2 and 100% relative humidity at 37 °C. Cells from a confluent monolayer were removed from flasks by a trypsin-EDTA solution (EuroClone). HBL-100 nontumorigenic epithelial cells were maintained in McCoy's 5A medium (SIGMA, St. Louis, MO, USA) supplemented with 10% FBS, 2 mM L-glutamine, 100 UI mL^{-1} penicillin, and 100 μg mL^{-1} streptomycin (EuroClone) in a humidified atmosphere with 5% CO_2 at 37 °C.

Cell viability was determined by the trypan blue dye exclusion test. For experimental purposes, the cells were sown in multi-well cell culture plastic plates (Corning Costar Italia, Milano, Italy). Cell growth was determined by the MTT viability test.[41] Cells were sown on 96-well plates and 24 h after showing were incubated with the appropriate compound at concentrations of 1–1000 μM, prepared by dissolving in a medium containing 5% of serum for 24, 48, and 72 h. Analysis was performed at the end of the incubation time. Briefly, MTT [3-(4,5-dimethylthiazol-2-yl)-2,5-diphenyltetrazolium bromide] dissolved in PBS (5 mg mL^{-1}) was added to all wells (10 μL per 100 μL of medium) and the plates were then incubated at 37 °C with 5% CO_2 and 100% relative humidity for 4 h. After this time, the medium was discarded and 100 μL of dmso (SIGMA) was added to each well according to the method of Alley and co-workers.[42] The optical density was measured at 570 nm on a SpectraCount Packard (Meriden, CT) instrument.

Supporting Information: ^{31}P NMR pH titration curves in D_2O for [RuCl(H_2O)(PTA)([9]aneS_3)]$^+$ (**4a**) and [RuCl(PTA)$_2$([9]aneS_3)][OTf] (**5**). UV/Vis spectral variations of [RuCl$_2$(PTA)[9]aneS_3] (**4**) in aqueous solution within 30 min after dissolution. ^1H NMR spectrum of [RuCl(en)([9]aneS_3)][OTf] (**6**) in CD_3NO_2. ^1H NMR spectra of [RuCl$_2$(PTA)([9]aneS_3)] (**4**), [RuCl(PTA)$_2$([9]aneS_3)][OTf] (**5**), [RuCl(en)([9]aneS_3)][OTf] (**6**), [RuCl(enac)([9]aneS_3)][OTf] (**7**), and [RuCl(bipy)([9]aneS_3)][OTf] (**8**) in D_2O, immediately after dissolution and after addition of 100 mM NaCl.

Acknowledgments

This work was performed within the framework of COST Action D20 (WG 0001 and WG 0005) and contributed by LINFA-MADE CRTrieste. We wish to thank Engelhard Italiana S.p.A. for a generous loan of hydrated $RuCl_3$.

[1] M. J. Clarke, *Coord. Chem. Rev.* **2003**, *236*, 209–233.
[2] a) B. K. Keppler, W. Rupp, U. M. Juhl, H. Enders, R. Niebl, W. Balzer, *Inorg. Chem.* **1987**, *26*, 4366–4370; b) B. K. Keppler, M. R. Berger, M. H. Henn, *Cancer Treat. Rev.* **1990**, *17*, 261–277.
[3] G. Sava, E. Alessio, A. Bergamo, G. Mestroni, in *Topics in Biological Inorganic Chemistry*, Vol. 1 "*Metallo-pharmaceutical*" (Eds.: M. J. Clarke, P. J. Sadler), Springer, Berlin, **1999**, pp. 143–169.
[4] a) E. Alessio, G. Mestroni, A. Bergamo, G. Sava, in *Metal Ions and Their Complexes in Medication and in Cancer Diagnosis and Therapy*, Vol. 42 of *Met. Ions Biol. Syst.* (Eds.: A. Sigel, H. Sigel), M. Dekker, New York, **2004**, pp. 323–351; b) E. Alessio, G. Mestroni, A. Bergamo, G. Sava, *Curr. Top. Med. Chem.* **2004**, *4*, 1525–1535.
[5] M. Galanski, V. B. Arion, M. A. Jakupec, B. K. Keppler, *Curr. Pharm. Des.* **2003**, *9*, 2078–2089.
[6] J. M. Rademaker-Lakhai, D. van den Bongard, D. Pluim, J. H. Beijnen, J. H. M. Schellens, *Clin. Canc. Res.* **2004**, *10*, 3717–3727.
[7] E. Reisner, V. B. Arion, M. F. C. Guedes da Silva, R. Lichtenecker, A. Eichinger, B. K. Keppler, V. Yu. Kukushkin, A. J. L. Pombeiro, *Inorg. Chem.* **2004**, *43*, 7083–7093.
[8] R. E. Morris, R. E. Aird, P. del Socorro Murdoch, H. Chen, J. Cummings, N. D. Hughes, S. Parsons, A. Parkin, G. Boyd, D. I. Jodrell, P. J. Sadler, *J. Med. Chem.* **2001**, *44*, 3616–3621.

[9] R. E. Aird, J. Cummings, A. A. Ritchie, M. Muir, R. E. Morris, H. Chen, P. J. Sadler, D. J. Jodrell, *Br. J. Cancer* **2002**, *86*, 1652–1657.
[10] a) H. Chen, J. A. Parkinson, S. Parsons, R. A. Coxall, R. O. Gould, P. J. Sadler, *J. Am. Chem. Soc.* **2002**, *124*, 3064–3082; b) H. Chen, J. A. Parkinson, R. E. Morris, P. J. Sadler, *J. Am. Chem. Soc.* **2003**, *125*, 173–186.
[11] O. Novakova, H. Chen, O. Vrana, A. Rodger, P. J. Sadler, V. Brabec, *Biochemistry* **2003**, *42*, 11544–11554.
[12] a) C. S. Allardyce, P. J. Dyson, D. J. Ellis, S. L. Heath, *Chem. Commun.* **2001**, 1396–1397; b) C. S. Allardyce, P. J. Dyson, *Platinum Met. Rev.* **2001**, *45*, 62–69.
[13] A. Dorcier, P. J. Dyson, C. Gossens, U. Rothlisberger, R. Scopelliti, I. Tavernelli, *Organometallics* in press.
[14] C. Scolaro, A. Bergamo, L. Brescacin, R. Delfino, M. Cocchietto, G. Laurenczy, T. J. Geldbach, G. Sava, P. J. Dyson, *J. Med. Chem.* in press.
[15] C. S. Allardyce, P. J. Dyson, D. J. Ellis, P. A. Salter, R. Scopelliti, *J. Organomet. Chem.* **2003**, *668*, 35–42.
[16] L. A. Huxham, E. L. S. Cheu, B. O. Patrick, B. R. James, *Inorg. Chim. Acta* **2003**, *352*, 238–246.
[17] D. N. Akbayeva, L. Gonsalvi, W. Oberhauser, M. Peruzzini, F. Vizza, P. Brüggeller, A. Romerosa, G. Sava, A. Bergamo, *Chem. Commun.* **2003**, 264–265.
[18] a) Y. N. Vashisht Gopal, D. Jayaraju, A. K. Kondapi, *Biochemistry* **1999**, *38*, 4382–4388; b) Y. N. Vashisht Gopal, N. Konuru, A. K. Kondapi, *Arch. Biochem. Biophys.* **2002**, *401*, 53–62.
[19] L. Dale, J. H. Tocher, T. M. Dyson, D. I. Edwards, D. A. Tocher, *Anti-Cancer Drug Des.* **1992**, *7*, 3–14.
[20] S. Korn, W. S. Sheldrick, *J. Chem. Soc., Dalton Trans.* **1997**, 2191–2199.
[21] S. Heeb, PhD dissertation, Ruhr-Universität Bochum, **1990**.
[22] a) S. R. Cooper, *Acc. Chem. Res.* **1988**, *21*, 141–146.
[23] a) M. Schröder, *Pure Appl. Chem.* **1988**, *60*, 517–524; b) A. J. Blake, M. Schröder, *Adv. Inorg. Chem.* **1990**, *35*, 1–80.
[24] a) C. Landgrafe, W. S. Sheldrick, *J. Chem. Soc., Dalton Trans.* **1994**, 1885–1893; b) K. Brandt, W. S. Sheldrick, *J. Chem. Soc., Dalton Trans.* **1996**, 1237–1243.
[25] a) S. Roche, C. Haslam, H. Adams, S. L. Heath, J. A. Thomas, *Chem. Commun.* **1998**, 1681–1682; b) S. Roche, H. Adams, S. E. Spey, J. A. Thomas, *Inorg. Chem.* **2000**, *39*, 2385–2390; c) S. Roche, S. E. Spey, H. Adams, J. A. Thomas, *Inorg. Chim. Acta* **2001**, *323*, 157–162; d) C. S. Araujo, M. G. B. Drew, V. Félix, L. Jack, J. Madureira, M. Newell, S. Roche, T. M. Santos, J. A. Thomas, L. Yellowlees, *Inorg. Chem.* **2002**, *41*, 2250–2259.
[26] a) B. J. Goodfellow, V. Félix, S. M. D. Pacheco, J. Pedrosa de Jesus, M. G. B. Drew, *Polyhedron* **1997**, *16*, 393–401; b) J. Madureira, T. M. Santos, B. J. Goodfellow, M. Lucena, J. Pedrosa de Jesus, M. G. Santana-Marques, M. G. B. Drew, V. Félix, *J. Chem. Soc., Dalton Trans.* **2000**, 4422–4431.
[27] a) X. Sala, I. Romero, M. Rodriguez, A. Llobet, G. González, M. Martinez, J. Benet-Buchholz, *Inorg. Chem.* **2004**, *43*, 5403–5409; b) X. Sala, A. Poater, I. Romero, M. Rodriguez, A. Llobet, X. Solans, T. Parella, T. M. Santos, *Eur. J. Inorg. Chem.* **2004**, 612–618.
[28] E. Iengo, E. Zangrando, E. Baiutti, F. Munini, E. Alessio, *Eur. J. Inorg. Chem.* **2005**, 1019–1031.
[29] This NMR feature is shared by all the following complexes (see Experimental Section) and will not be repeated in the text.
[30] N. W. Alcock, J. C. Cannadine, G. R. Clark, A. F. Hill, *J. Chem. Soc., Dalton Trans.* **1993**, 1131–1135.
[31] In general, for each complex, the manifold of multiplets of [9]aneS_3 also changes during hydrolysis but, owing to the diffused overlap of peaks, these resonances are difficult to use for monitoring the process.
[32] a) F. Wang, H. Chen, S. Parson, I. D. H. Oswald, J. E. Davidson, P. J. Sadler, *Chem. Eur. J.* **2003**, *9*, 5810–5820; b) R. Fernandez, M. Melchart, A. Habtemariam, S. Parsons, P. J. Sadler, *Chem. Eur. J.* **2004**, *10*, 5173–5179.
[33] The presence of two sets of resonances in the D_2O NMR spectrum of [RuCl(bipy)([9]aneS_3)]$^+$ (and of the analogous phen complex) was erroneously attributed by Goodfellow and coworkers to two different conformations of the thioether ring in slow equilibrium on the NMR timescale.[26a]
[34] P. J. Dyson, J. S. McIndoe, *Inorg. Chim. Acta* **2003**, *354*, 68–74.
[35] D. J. Daigle, A. B. Pepperman Jr., S. L. Vail, *J. Heterocycl. Chem.* **1974**, *11*, 407–408. .
[36] Z. Otwinowski, W. Minor, *Processing of X-ray Diffraction Data Collected in Oscillation Mode*, in *Methods in Enzymology, Volume 276: Macromolecular Crystallography, part A* (Eds.: C. W. Carter, Jr., & R. M. Sweet), Academic Press, **1997**, p.307–326.
[37] *SHELX97 Programs for Crystal Structure Analysis* (Release 97-2). G. M. Sheldrick, University of Göttingen, Germany, **1998**.
[38] *ORTEP3 for Windows*; L. J. Farrugia, *J. Appl. Crystallogr.* **1997**, *30*, 565.
[39] L. J. Farrugia, *J. Appl. Crystallogr.* **1999**, *32*, 837–838.
[40] P. Nanni, C. De Giovanni, P. L. Lollini, G. Nicoletti, G. Prodi, *Clin. Exp. Metastasis* **1983**, *1*, 373–385.
[41] T. Mosmann, *J. Immunol. Methods* **1983**, *65*, 55–63.
[42] M. C. Alley, D. A. Scudiero, A. Monks, M. L. Hursey, M. J. Czerwinski, D. L. Fine, B. J. Abbott, J. G. Mayo, R. H. Shoemaker, M. R. Boyd, *Cancer Res.* **1988**, *48*, 598–601.

Received: March 9, 2005
Published Online: June 21, 2005

